Supplementary information (SI)

Quantifiable models for surface protonic conductivity in porous oxides – case of monoclinic ZrO_2

Xinwei Sun,[a] ‡ Jie Gu,[b] ‡ Donglin Han,[b] * Truls Norby[a,b] *

[a] Department of Chemistry, University of Oslo, Centre for Materials Science and Nanotechnology (SMN), FERMiO, Gaustadalléen 21, NO-0349 Oslo, Norway

[b] College of Energy, Soochow University, No 1 Shizi Street, Gusu District, Suzhou, 215006, China

‡ Equal first authors

* Corresponding authors: dlhan@suda.edu.cn , truls.norby@kjemi.uio.no

SI 1 List of symbols and abbreviations

Table S1 Lists of symbols for variables and constants and abbreviations for sub- and subscripts.

Variables, constants	Unit	Description	Comment
a		Activity	
A		Geometric factor	
c_{BET}		BET constant	
c	mol/cm^3	Volume concentration	
C	F	Capacitance	
D	cm^2/s	Random diffusion coefficient	
d_g	cm	Grain and pore size	
E	kJ/mol	Heat of adsorption	Enters in c_{BET}
F	C/mol	Faraday constant	96485 C/mol
G	S	Conductance	
ΔH	kJ/mol	Enthalpy change	
K		Equilibrium coefficient	
l	cm	Length of surface layer sheet	
M		Metal	M = Ti, Zr, Ce…
M_m	g/mol	Molar mass	
p	bar	Partial pressure	
R	J/molK	Gas constant	8.3144 J/molK
R	ohm	Resistance	
RH		Relative humidity	$= p_{H_2O} / p_{ce}$
s	cm	Jump distance	
ΔS	J/molK	Entropy change	
SSA_g	cm^2/g	Specific surface area, gravimetric	
SSA_v	cm^2/cm^3	Specific surface area, volumetric	
SSA_m	cm^2/mol	Specific surface area, molar	

T	K	Absolute temperature	
t	cm	Thickness of surface layer	
u	cm^2K/Vs	Charge mobility	
w	cm	Width of surface layer sheet	
X		Site fraction	
Z	ohm	Impedance	
γ	mol/cm^2	Surface concentration	Gamma
ε_0	F/cm	Vacuum permittivity	$8.854 \cdot 10^{-14}$ F/cm
ε_e	F/cm	Effective dielectric constant	Epsilon
ε_r		Relative dielectric constant	Epsilon
θ		Surface coverage	Theta, = ν / ν_m
ν	mol/cm^2	Molar concentration of physisorbed water	Nu
ν_m	mol/cm^2	Molar concentration of a monolayer of water	Nu
ξ		Percolation power	Xi
ρ	g/cm^3	Density	Actual material
ρ_r		Relative density	Rho
ρ_t	g/cm^3	Theoretical density	Dense material
σ	S/cm	Conductivity	Sigma
ψ	1/cm	BLM porosity surface factor	Psi, = $\sigma_{M,s} / G_s$
ω_0	1/s = Hz	Vibrational attempt frequency	Omega
Subscripts			
1st level	2nd level		
a		adsorption	
	chm	chemisorbed molecular	
	chd	chemisorbed dissociative	
	ph1	1st physisorbed	
	ph2	2nd physisorbed	
d		dissociation	
	chm	in chemisorbed molecular layer	
	chm-s	from chemisorbed molecular layer to surface	
	chm-ph1	from chemisorbed molecular to 1st physisorbed	
	ph1	in 1st physisorbed layer	
m		migration	= diffusion
m,H^+		migration of H^+	Grotthuss
m,H_3O^+		migration of H_3O^+	vehicular in ph2
0		preexponential	like in u_0 and G_0
M		Macroscopic	like in σ_M
s		surface	like in G_s
L and Lp		One layer and one layer with effect of percolation	in $G_{s,L}$ and $G_{s,Lp}$
ce		condensation equilibrium	in p_{ce} and K_{ce}
r		relative	like in ρ_r and ε_r
geom		geometric	
cvex		convex	
cave		concave	
Superscript			
0		standard	like in p^0 and G^0

SI 2 Impedance spectra

Representative impedance spectra of samples sintered at low and high temperatures, measured at low and high temperatures, and in wet or dry atmosphere, are shown in Figure S1. The main

features are described in the main text, while we in SI 3 provide a more detailed assessment of the origin and parameters of the two high-frequency responses.

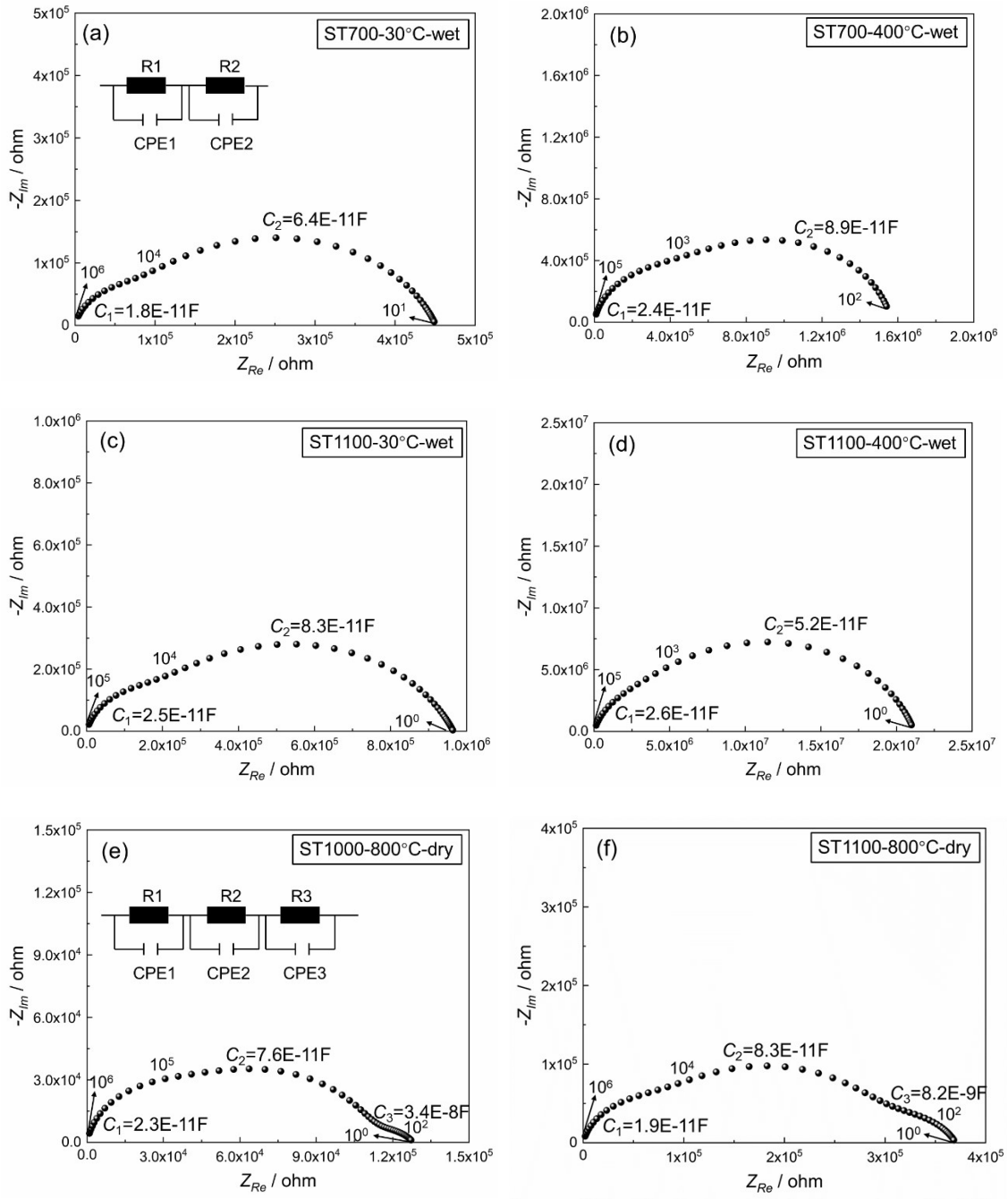

Figure S1. Impedance spectra ($-Z_{im}$ vs Z_{Re} in ohms) as measured at 30°C (a and c), 400°C (b and d) in wet (p_{H_2O} = 0.03 bar) Ar and at 800°C (e and f) in dry Ar for the samples sintered at 700°C (a and b), 1000°C (e), and 1100°C (c, d, f). The equivalent circuit used to model the data was either $(R_1Q_1)(R_2Q_2)$ in wet (exemplified in (a)) or $(R_1Q_1)(R_2Q_2)(R_3Q_3)$ in dry (exemplified in (e)). Numbers along the curve show the AC frequencies. Characteristic capacitances for the two or three responses are indicated (these include the parasitic capacitance of the ProboStat™ cell, which in the configuration used amounts to a few pF).

SI 3 Origin of the two high-frequency responses

The presence of two time constants associated with high frequencies and small bulk-like capacitances in these samples as well as in other porous ceramics with surface protonic

conduction could be attempted rationalised as due to intersecting grain boundaries or part of the electrode impedance. However, the high-temperature spectra in this study shows that the two high-frequency responses are well separated from the third response at lower frequencies that may be grain boundaries or electrodes. Moreover, the omnipresence of these dual time constants for all samples and conditions in this work and other studies of surface conduction in porous ceramics suggests that a more intrinsic phenomenon is at play.

Consider first two electrodes connected to a porous sample with no conductivity. It will have a dielectric response corresponding to the effective dielectric constant $\varepsilon_e = \varepsilon_{re}\varepsilon_0$ given by those of the gas phase (approximated by that of vacuum) and the ceramic phase, to a first approximation weighted by the relative density:

$$\varepsilon_{re} = 1 + (\varepsilon_r - 1)\rho_r \quad \text{and} \quad \varepsilon_e = \varepsilon_0(1 + (\varepsilon_r - 1)\rho_r) \qquad \textbf{Eq. 1}$$

For bulk monoclinic ZrO_2, the relative dielectric constant is approximately 20 [1], so that with 60% relative density, we will have $\varepsilon_{re} \approx 12$ and $\varepsilon_e \approx 10^{-10}$ F/m = 10^{-12} F/cm. Our samples with thickness 0.20 cm and electrode area 1.27 cm^2 would be expected to exhibit a geometric capacitance of $C_{geom} \approx 6 \cdot 10^{-12}$ F. With the addition of parasitic cell capacitance, this corresponds acceptably to the smallest capacitance responses in Figure SI 1.

If conduction would take place in the bulk of the grains, or along parallel surfaces, the response will be given by a simple circuit of the conductance and the capacitance in parallel, yielding a single bulk-like semicircle in a Nyquist plot. However, if the surface is curved, it will have convex features, like rounded and edged grains, and concave features, like grain necks. When the current passes over a convex feature, it will have a longer way to go in the conductive surface layer, but the parallel capacitance through the dielectric material of the grain gives this part of the transport a higher ratio between the parallel capacitance and the conductance compared to the average sample. In contrast, passing a concave part offers little capacitance from the gas phase there. Hence, the sample response would break up into a $(R_{cave}C_{cave})(R_{cvex}C_{cvex})$ type circuit, where the first part attributed to the concave features has low capacitance and high-frequency response, and the second one attributed to convex features has higher capacitance and a lower-frequency response. As an alternative, one may assign the geometric capacitance C_{geom} in parallel over a series connection of the concave part resistance and the parallel $(R_{cvex}C_{cvex})$ element: $(C_{geom}(R_{cave}(R_{cvex}C_{cvex})))$.

Deriving parameters from a simple 3D model microstructure is a mathematical exercise beyond the scope of this work. In reality, parameters are even more complicated to predict and analyse and may be expected to be dispersed due to variations in real microstructures. Hence, a very first step in this direction is to assign constant phase elements Q_{cvex} instead of C_{cvex} and use circuits $(R_{cave}C_{cave})(R_{cvex}Q_{cvex})$ or $(C_{geom}(R_{cave}(R_{cvex}Q_{cvex})))$.

Regardless of the difficulty to apply a geometrically correct model, the total surface resistance is $R_{tot} = R_{cave} + R_{cvex}$. We may furthermore predict that $R_{cvex}/R_{cave} > 1$ due to the long path around convex features compared with the short path across concave features like grain necks. In this work, the ratio is indeed typically 2-4. Somewhat larger ratios are being reported for porous

nanoscopic CeO_2 [2] while TiO_2 [3] with oriented grains have indications of larger ratios, that may reflect the sharper transitions between grains for materials crystallised rather than sintered.

The ratio between capacitances should be $C_{cvex}/C_{cave} > 1$, and predicted to reflect to a first approximation the ratio between the dielectric constant of the ceramic and the gas phase. The ratio of 2-4 in this work is considerably smaller, and we note that it is remarkably similar to the ratio of the resistances.

SI 4 Temperature dependence of conductivities

The temperature dependencies of the electrical conductivity extracted from the sum of resistances of the two high-frequency responses (as explained above) for all samples are shown in Figure S2.

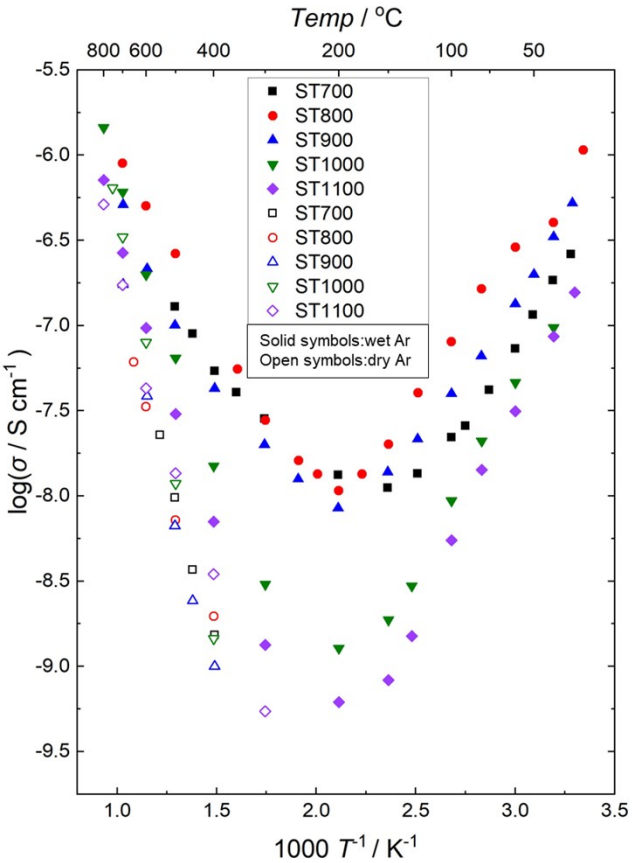

Figure S2 Plot of logσ vs 1/T in wet (p_{H_2O} = 0.03 bar) or bottle-dry Ar for samples sintered at different temperatures shown in the legend.

The results comprise samples manufactured and measured in the collaborating laboratories in China and Norway over a time span of several months, underlining the robustness of the temperature dependencies of the data.

Another sample ST800 was measured in wet O_2, and showed qualitatively the same conductivities and temperature dependencies as ST800 and the other samples measured in wet

Ar, suggesting that the oxygen partial pressure plays no significant role for ZrO_2, unlike what it does in CeO_2. [2, 4]

SI 5 Brick layer model (BLM) for surface conduction and SSA

Here, we first introduce briefly a simple brick layer model (BLM) for surface conduction in porous materials. Let us divide the volume of a porous material with equal grain diameters and pore diameters d_g into cubic bricks of the same size d_g so that there are $1/d_g$ bricks in each unit length direction and $1/d_g^2$ per unit area. The bricks are statistically grains or pores. We may count surfaces as belonging to grains or pores; we choose to count surfaces as belonging to grains. The chance that a brick is a grain is proportional to the relative density ρ_r.

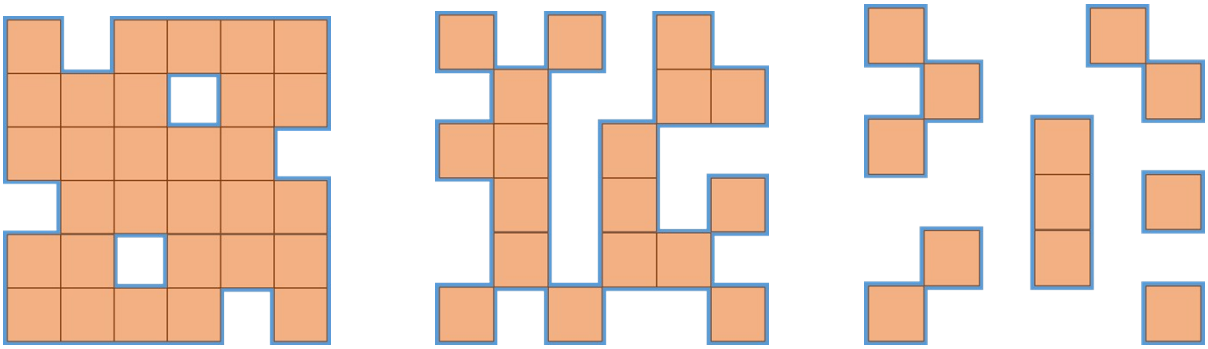

Figure S3. Schematic single layers of 6 x 6 brick "random" porous microstructures viewed from above, into the direction of conduction. Coloured bricks are grains, grain boundaries are thin black lines, surfaces with adsorbed water are thick blue lines. Densities are 5/6 (≈83%, left), ½ (50%, middle), and 2/3 (≈33%, right). Statistical numbers of conducting surfaces according to the model are, respectively, 20, 36, and 32 while actual numbers in a repeating matrix (counting only half the side surfaces) of these "random" examples of a small number of bricks are, respectively, 22, 45, and 36. Their overestimation of surfaces stems from the human rather than statistical selection of the microstructure.

In the direction of conduction, only 4 of the 6 sides (2/3) of a grain can contribute a conducting surface, and only if the neighbouring brick is a pore. For unit area of one layer of bricks, the number of grain side surfaces is thus $4\rho_r(1-\rho_r)/d_g^2$. This is a simple function that goes through a maximum of $1/d_g^2$ at 50% relative density $\rho_r = 0.5$. The surface conductance $G_{s,L}$ through one layer of bricks is obtained by multiplying with the side sheet surface conductance:

$$G_{s,L} = \frac{4\rho_r(1-\rho_r)}{d_g^2} G_s \qquad \textbf{Eq. 2}$$

Now, we consider the chance of percolation, i.e., the chance that a surface meets a new surface in the next layer. We take this to be the same that an interface is a surface, namely $\rho_r(1-\rho_r)$. Hence, the area specific number of connected conducting surfaces through one layer that percolates to the next is $4\rho_r^2(1-\rho_r)^2/d_g^2$. This is still a simple function with maximum at a relative density of 50%, now down at 0.25 conducting surfaces per brick, 0.5 per grain.

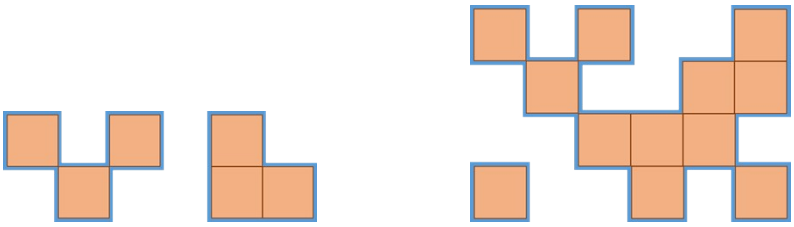

Figure S4. Schematic side views of the now vertical direction of conduction for examples of 2-layer (left) and 4-layer (right) brick structures both with 50% density. The 2-layer example shows that the top layer has 5 internal and one shared conducting surface, totalling at 5½, while the simple vertical percolation to the next layer restricts them to only 3. Statistically the model predicts a lowering by a factor of 4 for a case of 50% density in 2-dimesional brick planes, while for this 1-dimensional side-view case of only one brick thickness, the factor is expectedly 2. The 4-layer example (right) may help the reader evaluate how vertical percolation continues to restrict pathways, until there in this case is no vertical percolating paths, while horizontal surfaces continue to uphold conducting although longer paths.

We might continue like this, making the conduction path ever rarer, but orthogonal surfaces will immediately start to connect the ones we consider, and increase the conducting pathways. A numerical simulation of this could be useful, but the brick model is anyway crude. Generally, the power that the density and porosity are raised to, 1 and 2 in the above cases, can be a variable ξ in the surface conductance per layer of bricks taking percolation into account, $G_{s,Lp}$:

$$G_{s,Lp} = \frac{4\rho_r^{\xi}(1-\rho_r)^{\xi}}{d_g^2} G_s \qquad \textbf{Eq. 3}$$

In reality, an isotropic microstructure of high porosity such as for powder compacts or poorly sintered ceramics will have well-connected pores and ξ probably between 1 and 2, while low porosities and certain non-isotropic pore structures may be expected have ξ above 2.

A unit volume will have a conductance divided by the number of layers of grains, i.e., $1/d_g$, so that we get a macroscopic specific surface conductivity $\sigma_{M,s}$ for the porous material of

$$\sigma_{M,s} = \frac{G_{s,Lp}}{\frac{1}{d_g}} = d_g G_{s,Lp} = \frac{4\rho_r^{\xi}(1-\rho_r)^{\xi}}{d_g} G_s = \psi G_s \qquad \textbf{Eq. 4}$$

In this formula we recognise that the essential parameters are the conductance G_s of the surface layer (given by its volume specific conductivity and thickness), the relative density, and the grain (brick) size d_g.

The surface protonic conductivity of a simple porous material according to this model is inversely proportional to the grain size and has a maximum at 50% relative density of $\sigma_{M,s} = G_s/d_g$ for $\xi=1$ and $\sigma_{M,s} = 0.25 \cdot G_s/d_g$ for $\xi=2$.

The BLM handles in principle densities from 0 to 1 and to some extent closed porosity if $\xi>1$. In considering square bricks it underestimates conductivity by not allowing conduction along facets connecting otherwise unconnected grain sides. The BLM and the model proposed by Gregori *et al.* [5] model coincide well for $\xi=1$ (full percolation) at low porosities, while the BLM continues to handle the situation also as the porosity gets high.

From the geometry of porous ceramics, we may expect macroscopic conductivities to have shallow peaks around 50% density at values corresponding to order of magnitude of $\sigma_M = G_s/d_g$, i.e., the layer resistance in Siemens (S) divided by the grain size.

We next use the same BLM to make first approximation estimates of the specific surface area (*SSA*) of a porous material of the category we deal with here. In each layer of bricks there are 6 sides to each cube provided that the cube is a grain and its neighbour (in all 6 directions) is a pore. The number of surface sides per unit area of a layer is then

$$n_{6sL} = \frac{6\rho_r p_r}{d_g^2} = \frac{6\rho_r(1-\rho_r)}{d_g^2} \quad \textbf{Eq. 5}$$

The number of sides in a unit volume will be that of one layer have a surface area multiplied with the number of layers of grains, i.e., $1/d_g$;

$$n_{vs} = \frac{n_{6sL}}{d_g} = \frac{6\rho_r(1-\rho_r)}{d_g^3} \quad \textbf{Eq. 6}$$

The volumetric specific surface area SSA_v is then obtained by multiplying with the area of each side:

$$SSA_v = n_{vs} d_g^2 = \frac{6\rho_r(1-\rho_r)}{d_g} \quad \textbf{Eq. 7}$$

We may convert volumetric specific surface area SSA_v to gravimetric specific surface area SSA_g by

$$SSA_g = \frac{SSA_v}{\rho} = \frac{SSA_v}{\rho_r \rho_s} \quad \textbf{Eq. 8}$$

where ρ and ρ_r are, respectively, the density and relative density of the (porous) material, and ρ_s is the theoretical density of the dense material. We may also convert to molar specific surface area SSA_m by

$$SSA_m = \frac{SSA_g}{M_m} = \frac{SSA_v}{\rho_r \rho_s M_m} \quad \textbf{Eq. 9}$$

where M_m is the molar mass of the material.

References

1. Zhao, X. and D. Vanderbilt, *Phonons and lattice dielectric properties of zirconia.* Physical Review B, 2002. **65**(7): p. 075105.
2. Sun, X., Kalantzopoulos. N.G., Vøllestad. E., Chatzitakis, A, and Norby, T, *Surface protonic conductivity in chemisorbed and physisorbed water layers in porous nanoscopic CeO_2.* To be submitted.
3. Kang, X.L., et al., *Facet-engineered TiO_2 nanomaterials reveal the role of water-oxide interactions in surface protonic conduction.* Journal of Materials Chemistry A, 2022. **10**(1): p. 218-227.
4. Runnerstrom, E.L., et al., *Colloidal Nanocrystal Films Reveal the Mechanism for Intermediate Temperature Proton Conductivity in Porous Ceramics.* Journal of Physical Chemistry C, 2018. **122**(25): p. 13624-13635.

5. Gregori, G., M. Shirpour, and J. Maier, *Proton Conduction in Dense and Porous Nanocrystalline Ceria Thin Films.* Advanced Functional Materials, 2013. **23**(47): p. 5861-5867.